



## Iridium Barriers for Direct Copper Electrodeposition in Damascene Processing

D. Josell,<sup>a,z</sup> J. E. Bonevich,<sup>a</sup> T. P. Moffat,<sup>a,\*</sup> T. Aaltonen,<sup>b</sup> M. Ritala,<sup>b,\*</sup> and M. Leskelä<sup>b</sup>

<sup>a</sup>Metallurgy Division, National Institute of Standards and Technology, Gaithersburg, Maryland 20899, USA

<sup>b</sup>Laboratory of Inorganic Chemistry, University of Helsinki, Finland

Seedless superfilling by copper electrodeposition is demonstrated on submicrometer trenches with Ir barrier layers deposited by atomic layer deposition. The Cu deposition is seen to occur smoothly and continuously on the Ir without the benefit of a copper seed layer. The work supports efforts to develop diffusion barriers compatible with seedless superfill for damascene fabrication of interconnects. It also indicates the suitability of atomic layer deposition for fabrication of barrier layers, in this case Ir, for seedless processing.

© 2005 The Electrochemical Society. [DOI: 10.1149/1.2150165] All rights reserved.

Manuscript submitted August 17, 2005; revised manuscript received October 24, 2005.

Available electronically December 16, 2005.

As the width of on-chip interconnect wiring shrinks below 70 nm, a search is underway for new materials for the diffusion barrier between the electrically insulating dielectric and embedded signal-carrying, copper interconnects. The new materials must continue to prevent penetration of the copper interconnect material into the surrounding dielectric, a function presently accomplished by Ta and related barrier materials. In addition, the new barrier material must permit direct electrodeposition of copper without the use of the copper seed that is presently required due to poor nucleation of electrodeposited Cu on the surface oxide of conventional Ta barriers.<sup>1,2</sup> A variety of materials, including Ru, Pd, Pt, Rh, Ir, Ag, and Os have been suggested as possible replacement candidates for the barrier.<sup>3-6</sup> Copper superfill of sub-100 nm trenches with a barrier but without a Cu seed has been demonstrated only for Ru and Os barriers.<sup>4,6</sup> Significantly, recent studies of Cu/Ru thin films suggest that, by itself, Ru is not capable of preventing copper leakage into the dielectric during processing;<sup>7-9</sup> it has yet to be determined if Os is better (though there are reasons to suspect it might be<sup>6</sup>). This paper examines deposition in trenches with an Ir barrier in order to determine whether seedless superfill by direct copper deposition is also possible with this system.

### Experimental

Lithographically patterned SiO<sub>x</sub>/Si wafers were provided by International Sematech. Prior to Ir deposition, several nanometers of amorphous alumina were deposited on the substrates as an adhesion layer using an atomic layer deposition (ALD) process involving trimethyl aluminum and water. The Ir ALD deposition process has been described previously.<sup>10</sup> The barrier in the field and within the trench is highly conformal and ~10 to 15 nm thick as expected for 200 and 300 ALD cycles, respectively.<sup>10</sup>

Copper electrodeposition was conducted after transatlantic shipment of the Ir coated substrates, and occurred between 3 and 5 days after the Ir depositions. Copper depositions were performed in an electrolyte comprised of 1.8 mol/L H<sub>2</sub>SO<sub>4</sub> + 0.24 mol/L CuSO<sub>4</sub> to which additives required for superfill, specifically 1 mmol/L NaCl + 88 μmol/L PEG (polyethylene glycol, 3400 Mw) and

50 μmol/L SPS (Na<sub>2</sub>[SO<sub>3</sub>(CH<sub>2</sub>)<sub>3</sub>S]<sub>2</sub>, Raschig),<sup>c</sup> were added. Specimens were cross sectioned after deposition and examined by field-emission scanning electron microscopy (SEM) and transmission electron microscopy (TEM) to assess the trench filling.

Conduction through the thin Ir barrier layers was accompanied by an IR voltage drop during electrodeposition. This so-called "terminal effect" influences deposit morphology through the potential-dependent nature of the copper deposition process; it can also be convoluted with potential-dependent oxide removal as has been noted previously with Ru.<sup>11</sup> No attempt was made to control this effect in these demonstration experiments; the electrical contact clip was in a region that was not placed in the electrolyte and was ~1 cm from the region of the die sectioned for the study. Based on the specimen geometry (i.e., the 1 cm<sup>2</sup> immersed specimen area and ≈1 cm distance between the contact and immersed region), an estimated 4 mA/cm<sup>2</sup> current density, a 10 nm Ir film thickness and 10 μΩ cm Ir resistivity,<sup>10</sup> the IR drop across the unplated region is expected to be 40 mV.

Previous work in the area of seedless copper superfill using Ru has revealed a sensitivity of filling behavior to the manner in which the Ru barrier layer was treated prior to plating.<sup>11</sup> Copper deposition was noted to depend substantially on the oxidation state of the Ru surface. Processes for remediation of the oxidized barrier, by reducing the native oxide prior to or concurrent with copper deposition, have been described in studies with both Ru and Os barriers. Only preliminary results obtained using an unoptimized process are described in this paper.

### Results and Discussion

Figure 1 shows the filling of trenches of five different widths on two different specimens, both specimens after the identical process of 30 s at 0.1 V SCE (saturated calomel electrode), 1 s at -0.4 V SCE, and 40 s at -0.2 V SCE. The specimen was immersed at the initial potential. The nominal intent of the three steps in this sequence were to permit underpotential deposition (upd) of copper along with adsorption of superfilling additives on the Ir surface, nucleate a high density of Cu grains, and deposit the Cu at a potential where interface charge transfer kinetics, rather than diffusional transport, would be important. It has not been established whether the individual steps of the process acted as intended.

The Ir barriers are evident as bright layers beneath the Cu deposits in Fig. 1; the top specimen has an Ir barrier fabricated using 300 ALD cycles while the barrier on the bottom specimen involved 200 ALD cycles. Delamination between the ALD barrier and the underlying dielectric, evident in the field near the large trench in Fig. 1,

\* Electrochemical Society Active Member.

<sup>z</sup> E-mail: daniel.josell@nist.gov

<sup>c</sup>Product names are included only for accuracy of experimental description. They do not imply NIST endorsement.

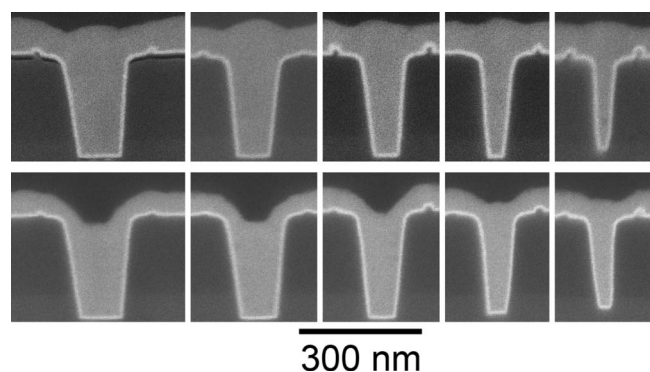


**Figure 1.** Cu deposition in trenches of five different widths as viewed by SEM. Cross sections are shown from two cross-sectioned specimens: (top) 300 cycle ALD Ir barrier and (bottom) 200 cycle ALD Ir barrier. The bottom-up filling and overfill bump associated with the superfill phenomenon are evident. Delamination between the ALD Ir barrier and the underlying  $\text{SiO}_x$  dielectric is visible under the widest trench (top).

likely occurred during the grinding and polishing associated with the cross sectioning process. Importantly, delamination was not observed between the Ir and Cu. Consistent with superfilling, trenches with widths from above to well below 100 nm are fully filled with neither seams nor voids. They also exhibit overfill bumps above the features as well as unambiguous bottom-up filling, both of which are well known manifestations of the superfill phenomenon. The small difference between the two specimens is likely a result of different IR drops due to the different Ir film thicknesses. In both cases, the Cu electrodeposit is significantly thinner than is typical for the same electroplating conditions on physical vapor deposited (PVD) Cu, Ru or Os surfaces.<sup>4,6,11</sup> This difference is likely due to the substantial excess seed layer thickness of PVD films that is required to obtain the desired sidewall thickness; this decreases the IR voltage drop described earlier. Figure 2 shows filling of a much wider trench from the same specimen and region as that from which the upper images in Fig. 1 were obtained; the enhanced deposition in the bottom corners is an additional manifestation of the superfill phenomenon.<sup>12</sup>

Figure 3 shows a TEM image of the wider trenches that confirms the seam-free filling of the trenches. The conformality of the ALD process for the barrier is also evident in the uniform thickness of the Ir layer within the trench and on the field; most striking is the semi-cylindrical deposit around the dielectric protrusions (artifact) in the field adjacent to the trenches. The TEM images were obtained from the same specimens shown in Fig. 1 except that they were obtained, after additional thinning to reach electron transparency, approximately 21 months after the SEM images in Figs. 1 and 2. Large grains typical of a recrystallized Cu deposit, such as is expected after more than a few days as a result of the well-known room temperature process, are evident. Figure 4 shows a higher magnification view of the trench marked with an arrow in Fig. 3. The inset shows a compositionally sensitive map of the Al  $L_{2,3}$  edge (jump

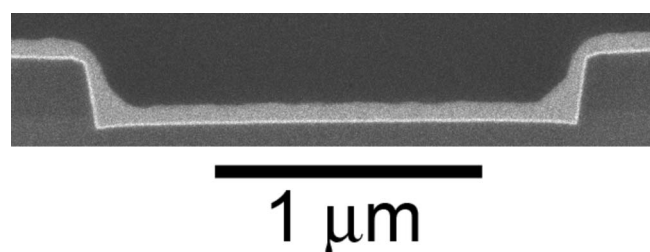


**Figure 2.** Cu deposition in a very wide trench on the same specimen as Fig. 1 (top) as viewed by SEM. The enhanced deposition at the bottom corners is a manifestation of superfill.

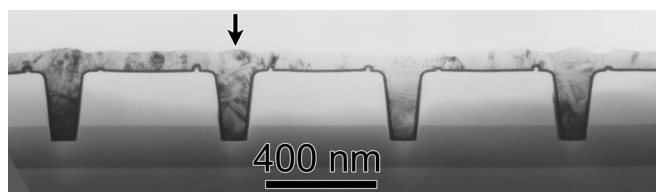


**Figure 3.** Cu deposition in  $\approx 100$  nm wide trenches [specimen of Fig. 1 (top)] as viewed by TEM after a 21 month delay. Large Cu grains, typical of recrystallized deposits from superfilling electrolytes after more than a few days at room temperature, are visible. The Ir barrier is seen to be highly conformal, even duplicating the semi-cylindrical protuberances running parallel and adjacent to the trenches on the field of the patterned  $\text{SiO}_x$ .

ratio) obtained by dividing electron inelastic scattering yields at energies slightly greater ( $78 \pm 5$  eV) and less ( $66 \pm 5$  eV) than that of the aluminum  $L_{2,3}$  edge at 73 eV. The alumina adhesion and Ir barrier layers are distinctly visible, the alumina adhesion layer showing as a bright region between the Ir barrier and patterned  $\text{SiO}_x$  due to the discontinuity of electron yield exhibited by Al because of this energy edge. Roughness of the Cu/Ir interface (several nanometers) is clearly visible in the composition map. The possibility of diffuseness of the alumina/Ir interface suggested in the map cannot be ruled out.

Figure 5 shows SEM images of a specimen cross-sectioned after 5 s at 0.1 V SCE, 1 s at  $-0.4$  V SCE and 10 s at  $-0.2$  V SCE; note the shorter pretreatment and deposition times. Smooth, continuous deposition across the specimen surface, characteristic of good nucleation and wetting, is evident. Enhanced deposition in the bottom corners of the trenches is also apparent.

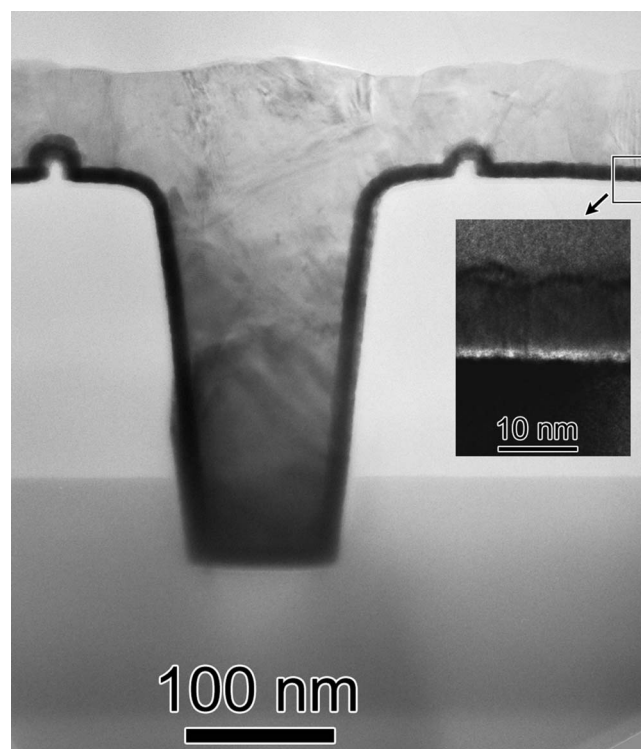


**Figure 4.** A higher magnification view of the trench in Fig. 3 indicated by the arrow. A compositionally sensitive map has been inserted. The alumina adhesion layer appears as a bright layer immediately below the Ir barrier.

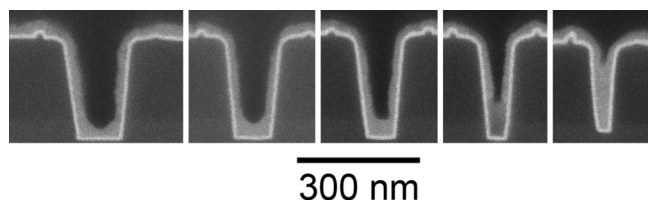


**Figure 5.** Cu deposition in trenches of five different widths as viewed by SEM. Effective wetting and enhanced Cu deposition at the bottom corners, the latter associated with the superfill phenomenon, are both evident.

### Conclusions

Seedless superfilling of submicrometer trenches with iridium barriers by direct copper electrodeposition was investigated. The results demonstrate that iridium barriers, like ruthenium and osmium, permit copper wetting and superfill during electrodeposition without the need for a copper seed layer. While the slight mutual solubilities of Ir and Cu might preclude the use of elemental Ir as a barrier material, this work supports the goal of seedless processing for damascene interconnect fabrication.

The National Institute of Standards and Technology assisted in meeting the publication costs of this article.

### References

1. A. Radisic, Y. Cao, P. Taephaisitphongse, A. C. West, and P. C. Searson, *J. Electrochem. Soc.*, **150**, C362 (2003).
2. A. Radisic, G. Oskam, and P. C. Searson, *J. Electrochem. Soc.*, **151**, C369 (2004).
3. O. Chyan, T. N. Arunagiri, and T. Ponnuswamy, *J. Electrochem. Soc.*, **150**, C347 (2003).
4. D. Josell, D. Wheeler, and T. P. Moffat, *Electrochem. Solid-State Lett.*, **6**, C143 (2003).
5. M. W. Lane, C. E. Murray, F. R. McFeely, P. M. Vereecken, and R. Rosenberg, *Appl. Phys. Lett.*, **83**, 2330 (2003).
6. D. Josell, C. Witt, and T. P. Moffat, *Electrochem. Solid-State Lett.*, **9**, C41 (2005).
7. R. Chan, T. N. Arunagiri, Y. Zhang, O. Chyan, R. M. Wallace, M. J. Kim, and T. Q. Hurd, *Electrochem. Solid-State Lett.*, **7**, G154 (2004).
8. T. N. Arunagiri, Y. Zhang, O. Chyan, M. El Bouanani, M. J. Kim, K. H. Chen, C. T. Wu, and L. C. Chen, *Appl. Phys. Lett.*, **86**, 083104 (2005).
9. H. Kim, T. Koseki, T. Ohba, T. Ohta, Y. Kojima, H. Sato, and Y. Shimogaki, *J. Electrochem. Soc.*, **152**, G594 (2005).
10. T. Aaltonen, M. Ritala, V. Sammelselg, and M. Leskela, *J. Electrochem. Soc.*, **151**, G489 (2004).
11. T. P. Moffat, M. Walker, P. J. Chen, J. E. Bonevich, W. F. Egelhoff, L. Richter, C. Witt, T. Aaltonen, M. Ritala, M. Leskelä, and D. Josell, *J. Electrochem. Soc.*, **153**, C37 (2005).
12. T. P. Moffat, D. Wheeler, M. D. Edelstein, and D. Josell, *IBM J. Res. Dev.*, **49**, 19 (2005).